Surface energy determination of fibres for Liquid Composite Moulding processes: method to estimate equilibrium contact angles from static and quasi-static data

William Garat, Monica Francesca Pucci, Romain Léger, Quentin Govignon, Florentin Berthet, Didier Perrin, Patrick Ienny, Pierre-Jacques Liotier

Surface energy determination of fibres for Liquid Composite Moulding processes: method to estimate equilibrium contact angles from static and quasi-static data

William GARAT[1], Monica Francesca PUCCI[2], Romain LEGER[2], Quentin GOVIGNON[4], Florentin BERTHET[4], Didier PERRIN[3], Patrick IENNY[2], Pierre-Jacques LIOTIER[1]

[1] *Mines Saint-Etienne, Université de Lyon, CNRS, UMR 5307 LGF, Centre SMS, 158 Cours Fauriel – 42023 Saint-Etienne, France*

[2] *LMGC, IMT Mines Ales, Univ Montpellier, CNRS, Ales, France*

[3] *Polymers Composites and Hybrids (PCH), IMT Mines Ales, Ales, France*

[4] *Institut Clément Ader (ICA) ; Université de Toulouse ; CNRS, IMT Mines Albi, INSA, ISAE-SUPAERO, UPS ; Campus Jarlard, F-81013 Albi, France*

Abstract

Interest in eco-composites incorporating elements from recycling is growing to reduce the carbon footprint of final products. Therefore, the characterisation surface properties of recycled fibres is of first importance. However, in order to maximise the service properties and facilitate their development, chemical surface treatments can be made in order to improve fibres compatibility with resins. For a better understanding of the behaviour of these new reinforcements during Liquid Composite Moulding processes (LCM), surface analysis and wetting properties are studied. However, this type of analysis, using the Owens and Wendt relation and based on tensiometric methods, requires special procedures, specifically for estimation of the contact angle. Based on two tensiometric methods, carbon and basalt fibres with different sizing are characterised in first approach, in order to be able to address recycled materials in further studies. The main contribution of this study is to evaluate the error in surface energy and its components determination associated to the measurement of an alleged equilibrium contact angle deriving from static or quasi-static data.

Keywords

A. Fibres; B. Wettability; E. Liquid Composite Moulding; D. Surface analysis.

1. Introduction

Mechanical properties of final composite materials are not only controlled by the intrinsic properties of resin and fibres, but also by the compatibility between them and more precisely by the fibre wetting during Liquid Composite Molding (LCM). Those parameters indeed control the final void content and interfacial properties of the composite parts. Fibre surface chemistry and morphology affect wetting properties [1]. Therefore, the surface properties of fibres affect their impregnation during manufacturing and thus directly the quality of the fibre / matrix adhesion. To improve compatibility with the resin (thermoplastics and / or thermosets) various treatments to modify the surface properties have been investigated in literature, whether thermal, mechanical or chemical [2–5]. However, the methods used to characterize the fibre surface energy after modification and also considering the effect of sizing, are not always consistent with the physical meaning of wettability [6][7]. Indeed, the determination of surface energies and then their compatibility in terms of wetting requires the identification of their polar and dispersive components. Unlike the surface tension of liquids (which can be determined with Wilhelmy plate method [8]), the determination of the fibre surface energy and components cannot be obtained directly. It follows from the Owens and Wendt law [7] combined with the equilibrium Young relation [9] which takes into account measurements of an equilibrium contact angle θ_e for each fibre/liquid couple. In literature, different studies focused on wettability of synthetic [10–15] and natural fibres[16]. However, independently of the fibre considered, current methods to measure contact angles on single fibres imply some reproducibility issues that make results of surface energy measurements unreliable and difficult to compare [7][17]. We can notably mention the drop shape analysis method [18,19] (using a goniometer) and the Wilhelmy plate method (using a tensiometer) [6]. This latter appears the most convenient for the measurement of

contact angles, especially for singles fibres, to gather also information about impregnation in static and dynamic conditions [11,15,20,21]. Some of those studies consider the theoretical static contact angle while others consider advancing and/or receding contact angle. Differences in angles considered induce very large errors in calculation of the surface energy and components. This difficulty in accurately measuring the static angle leads to misunderstanding of the results inducing some errors on the affinity with liquids.

In this work, a comparative analysis of methods to measure the static contact angle was made. Based on two tensiometric methods from two laboratories, i.e. using the K100SF tensiometer from KRÜSS in IMT Mines Alès and the DCAT11 tensiometer from Dataphysics in IMT Mines Saint-Etienne, static, advancing and receding contact angles were determined and treated according to a linear regression method previously developed [22]. It is important to note that the aim of this study is not to compare equipments but to validate both methods or a crossover of the two methods. To facilitate the experimental procedure, the basalt and carbon fibres, having relatively homogeneous and reproducible morphologies, were selected. Finally, the different contact angles were associated with the Owens and Wendt equation in order to evaluate the measurement errors in each type of fibre surface energy determination.

2. Experimental section

2.1. Materials

2.1.1. Basalt and carbon fibres

Three types of fibre, presenting controlled morphologies with circular section were chosen to correlate tensiometric methods. Two types of basalt fibre having different types of sizing compatible with thermoset resins were tested. The first one, basalt

fibres extracted from TX520 triaxial stitched fabrics provided by Basaltex are characterised by a silane-based sizing compatible with epoxy. Those fibres will be referred to as Basalt TX520. The second one, basalt fibres extracted from B400 triaxial stitched fabrics provided by Basaltex has a sizing agent compatible with vinylester resin. Those fibres will be referred to as Basalt B400. Carbon fibre was also chosen because of its intensive use in composite materials made by LCM processes. Carbon fibres were extracted from Cbx600 fabrics (provided by Sicomin) with12K yarns, and a nominal Tex of 1850 and a sizing agent compatible with epoxy. The areal weight is of 629 ± 5% g/m² and the nominal diameter is of 6µm with deviation lower than 0.5µm over 20 fibres.

Some basalt and carbon single fibres extracted from fabrics were tested to characterise contact angles and determine their surface energies and components by Owens and Wendt method [23].

2.1.2. Test liquids for wetting analysis

Four liquids were used in this study for wetting analysis: n-hexane, water and two resins. Their characteristics at room temperature of 20°C are listed in **Table 1**, i.e. the surface tension γ_L, the polar γ_{L}^{p} and dispersive $\gamma_{\mathrm{L}}^{\mathrm{d}}$ components and the viscosity η. The n-hexane was chosen as totally wetting liquid, because of its low and totally dispersive surface tension (18.4 mN/m) for which the contact angle can be theoretically considered as null (θ_e = 0°). Conversely, the water is used as the most common liquid with a high polar component (51.0 mN/m) and surface tension (72.8 mN/m). Then, two thermoset resins which cure rapidly at room temperature, i.e. the epoxy *SP106*® provided by Gurit and the vinylester *Altac E-Nova*® *MA6215* provided by DSM Composite Resins, were also chosen because their formulations are the most commonly used for LCM processes. The uncured resin characteristics were determined according to the procedure described by **Pucci et al.** [22]. As in this

previous work, only the base (not the catalyst or hardener) of those resins has been used in order to avoid polymerisation and time dependant changes in the fluids properties. Furthermore, as in previous study [22], the surface tension is considered as barely affected by the mixing in of the hardener with only a negligible change of the polar component of the liquid resin..

Table 1. Characteristics of liquids and resins at 20°C [22,24,25]

	η (mPa s)	γ_L^p (mN/m)	γ_L^d (mN/m)	γ_L (mN/m)
n-Hexane	0.32	0.0	18.4	18.4
Water	1.00	51.0	21.8	72.8
SP106 (epoxy)	1360	4.5 ± 0.5	35.8 ± 0.5	40.3 ± 1
Altac E-nova (vinylester)	80-90	4.0 ± 0.1	31.7 ± 0.6	35.7 ± 0.7

2.2. Methods

2.2.1. Fibre surface characterisation

A Scanning Electron Microscope (SEM) was used (6500F from JEOL) to evaluate the surface morphology of basalt and carbon single fibres and determine their diameters. The mean nominal diameter based on the measurement of 20 apparent diameters (4 measurements by fibre on 5 fibres) for each batch of single fibre was used the study.

2.2.2. Tensiometric characterisation of contact angles

Tensiometric methods appear as the most convenient for the measurement of contact angles especially for singles fibres to gather also information about impregnation in static and dynamic conditions [11,15,20]. Tensiometer measures the capillary force corresponding to the meniscus mass *m* formed by the liquid around fibres [26]. During measurements, fibres are suspended as vertically as possible in a stationary position and the vessel holder moves up (advancing phase) and down

(receding phase) (**Figure 1.a**). Between the advancing and receding phases, the vessel holder is stopped for 60s to make sure the liquid meniscus around the fibres reached a static configuration. Based on these capillary force measurements and knowing the fibre perimeter *p* (by SEM) and the surface tension of the liquid (**Table 1**), values of static (θ_s), advancing (θ_a) and receding (θ_r) contact angles can usually be derived from the Wilhelmy relationship:

$$F_c = ma = p\gamma_L \cos\theta \quad (1)$$

where F_c is the capillary force, a the acceleration due to gravity and θ the contact angle related to the phase of test. The buoyancy effect is here neglected due to the very small volume of the fibres, the induced force would be lower than the devices resolutions.

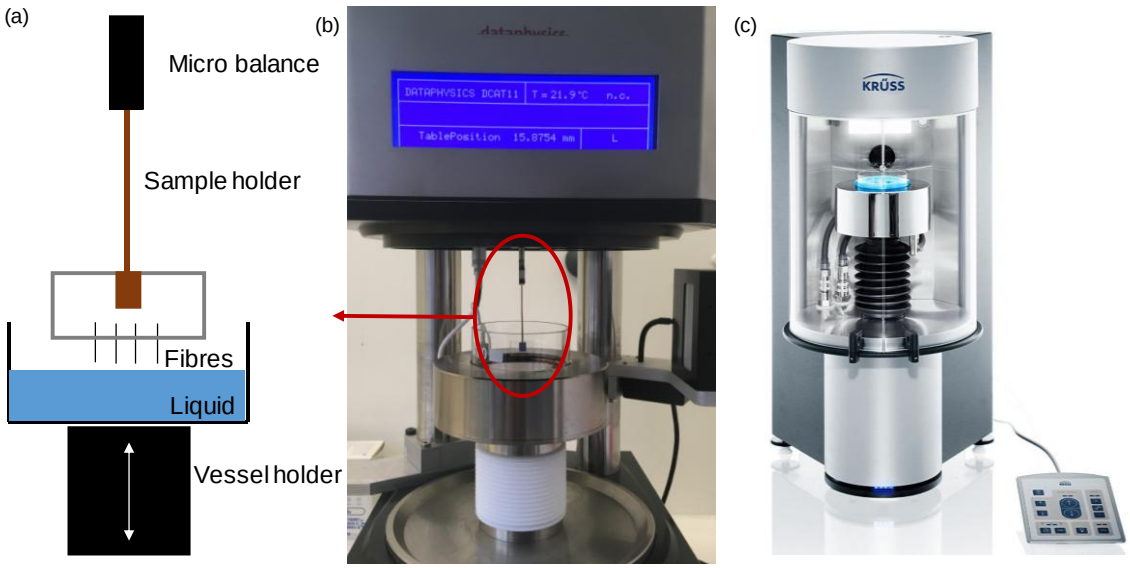

Figure 1. (a) Schematic representation of the vertical mounting of four fibres during testing, (b) DCAT11 tensiometric device and (c) K100SF tensiometric device.

In this study, two tensiometric methods were compared and combined to determine contact angles.

The first method uses the DCAT11 tensiometer (Dataphysics Instrument GmbH, Fildesadt) with a resolution of 10^{-5} g (referred as “standard tensiometer” - **Figure**

1.b). Different numbers of fibres were clamped to the tensiometer (2 fibres, 3 fibres or 4 fibres) to compensate for the small single fibre mass of the formed meniscus (example of four fibres in **Figure 1.a**). A specific immersion depth of 3 mm (fibres have thus to be longer than 3 mm) and a low immersion and withdrawal speed of 0.01 mm/s were set. During tests, fibres were maintained in static position for 60 s after immersion to determine a representative value of meniscus mass at static conditions [27]. These conditions have already been validated in previous laboratory works [22,28]. Examples of complete cycles for B400 basalt fibres wetted by the SP106 resin are shown on **Figure 2**. At the beginning of the test, the force is set to zero. During the advancing phase, each detected fibre corresponds to a force jump to a higher steady value. Then, a higher steady state per value is observed, which corresponds to the static phase during 60s. After this one, the receding phase occurs. During the receding phase each detected drop in force corresponds to the withdrawal of a fibre from the liquid until total withdrawal. Based on the meniscus mass measurement and following the Wilhelmy relationship (Eq. **(1)**) the fibre/liquid contact angle can be obtained by plotting the capillary force F_c (mN) as a function of the wetted length p (m). Therefore, the increase in the number of fibres increases the wetted length of the tested solid and then the capillary force varies linearly. According to these considerations, θ_s will be calculated from linear regression method previously developed [22]. Besides the static contact angle measurement, advancing (considering the mean capillary force over the last 60 seconds) and receding (considering the mean capillary force over the first 60 seconds) angles were also measured. It is also possible to determine for each phase (advancing, static and receding) a representative value of θ_a and θ_r per liquids.

The second method uses the K100SF tensiometer (Krüss GmbH, Hamburg, Germany) with a resolution of 10^{-7} g (referred as “single fiber tensiometer” - **Figure**

1.c). During tests, each single fibre was maintained in static position for 60 s after immersion to determine a representative value of meniscus mass [27]. Qiu et al. [29] suggested that dynamic advancing contact angles measured below 20 mm/min can be recognized as static advancing contact angles. In the present study, a specific immersion depth of 5 mm and a low immersion and withdrawal speed of 0.01 mm/s were set. An example of a complete cycle for one B400 basalt fibres wetted by the SP106 resin test is shown on **Figure 3**. The first part of the curve, from 0 to 1.3mm (corresponding to the point A), represents the measurement before touching the liquid and highlights a drift in the force which must be taken into account to minimize the error, since this drift is significant but not repeatable. This drift is partially due to the adsorbtion of volatile molecules on the tested sample. This is why no adhesive tape or glue should be used for this test. The fibre is thus clamped in an adapted pliers attached to the tensiometer. After contact with the liquid (point B), the curve is related to the capillary process of meniscus formation and advancing phase up to the point C, corresponding to the beginning of the static phase of 60 seconds. The dynamic advancing contact angle θ_a can be measured here considering the capillary force at the point C from which the drift in the capillary force corresponding to the point A is subtracted. During the immersion until a displacement distance of 5 mm, a decrease in capillary force could occur due to buoyancy effects [29]. For single fibres with low diameters, as in Fig. 3, this effect can be neglected [16], even for the use of four fibres. The second part of the curve corresponds to the receding phase until the point E, which represents the fibre extracted from the liquid. The dynamic receding contact angle θ_r can be obtained considering the capillary force at point D from which the drift in the capillary force corresponding to point A is subtracted. The static contact angle θ_s was then calculated here from the average of the sum of receding

and advancing capillary forces (C and D points) which the drift in the capillary force corresponding to point A is subtracted [33].

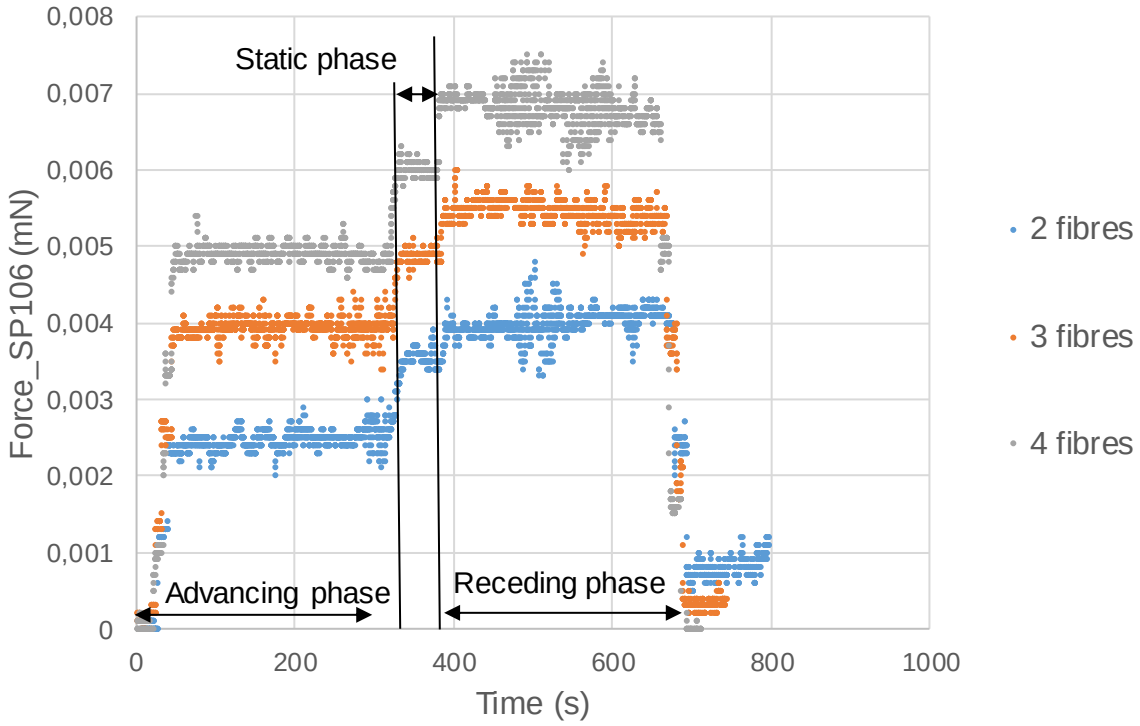

Figure 2. Example of a complete cycle for two, three and four B400 basalt fibres in SP106 resin with the DCAT11 tensiometer.

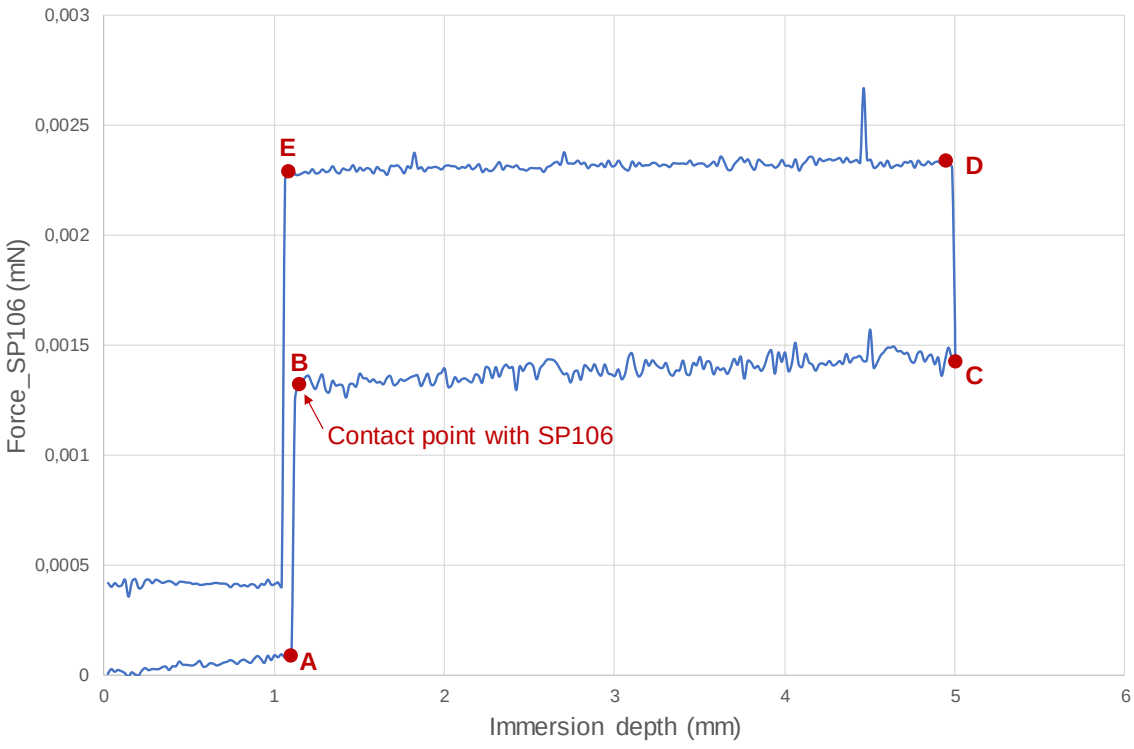

Figure 3. Example of a complete cycle for one B400 basalt fibre in SP106 resin with the K100SF tensiometer.

For calculation of surface energies, the advancing, the receding and the static capillary forces where considered to calculate the relative angles through Wilhelmy relationship (Eq**. (1)**). For each fibre (basalt or carbon), each number of fibre (1 fibre with the K100SF and 2,3,4 fibres with the DCAT) and each specific liquid, five tests were carried out in order to obtain the minimum dispersion.

It is important to specify here that dynamic measurements induce a modification of the contact angles along with the fluid velocity (that can be related to the associated adimensional capillary number [21-36]). Since the fluid velocity has been set to 1mm/min, it can be assumed that the advancing and receding angles are quasi-static. It is thus considered in this work that the advancing and receding angles are the static advancing and static receding for each solid/liquid couple.

2.2.3. Characterisation of fibre surface energy

The Owens and Wendt method based on the equation (2) [23] and coupled with the contact angle defined by the Young-Laplace equilibrium (Eq. (3)) [9] can be used to determine dispersive and polar components of surface energy for basalt and carbon fibres.

$$\gamma_s + \gamma_L - \gamma_{sL} = 2(\gamma_S^d \gamma_L^d)^{0.5} + 2(\gamma_S^p \gamma_L^p)^{0.5} \quad (2)$$

$$\cos\theta_e = \frac{\gamma S - \gamma SL}{\gamma L} \quad (3)$$

where γ_S, γ_L and γ_{SL} are the surface energies of respectively the solid, the liquid and the solid/liquid interface, γ_S^d and γ_S^p are respectively the dispersive and the polar components of surface energy of the solid and θ_e refers to the equilibrium contact angle defined by equation 3. γ_S is equal to the sum of dispersive and polar components. It is possible to determine both components of surface energy using at

least a minimum of two liquids [20][7], including a totally dispersive one [30]. Values of contact angle for each liquid were estimated in three conditions as well: static, advancing and receding condition (section 2.2.2.). Four liquids including vinylester and epoxy resins were used in addition to the theoretical contact angle of 0° given by the n-Hexane (**Table 1**). Owens and Wendt equation can then be rewritten as follows:

$$\underbrace{\frac{\gamma_L\,(1+\cos\theta e)}{2\sqrt{\gamma_L^d}}}_{Y} = \underbrace{\sqrt{\gamma_S^p}\left(\frac{\sqrt{\gamma_L^p}}{\sqrt{\gamma_L^d}}\right)}_{X} + \sqrt{\gamma_S^d} \qquad (4)$$

Considering the left hand-side term as the Y ordinate, and the fraction in brackets in the right hand-side term as the X abscissa, the slope and the y-intercept of the linear fit are respectively the square roots of polar and dispersive components.

3. Results

3.1. Fibres surface morphology characterisation

Figure 4 shows SEM micrographs of the carbon fibre and the two types of basalt. The obvious information concerns the different surface morphology of basalt fibres compared to carbon fibre. Sizing agent treatments are clearly visible on the surface on both types of basalt fibres, which present equivalent surface morphology with residue of sizing. Moreover, basalt fibres have a higher diameter than carbon fibres.

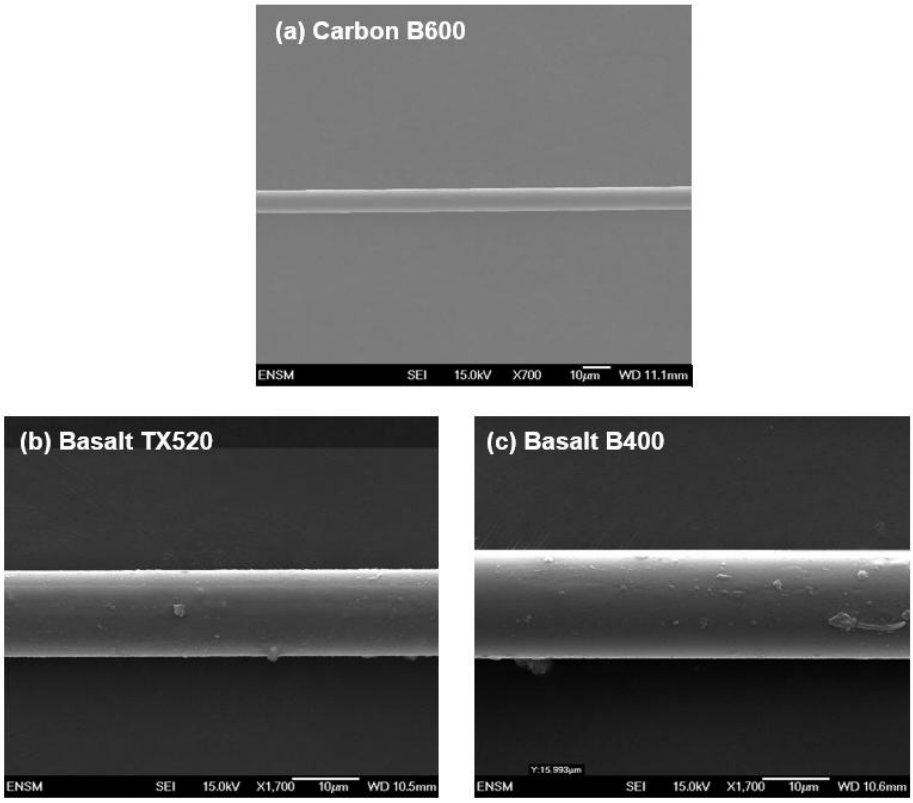

Figure 4. SEM micrographs of (a) raw carbon fibres and basalt fibres with sizing agents for (b) epoxy and (c) vinylester.

3.2. Determination of contact angles

The results of tests carried out with the K100SF tensiometer for one single fibre and the DCAT11 tensiometer for two, three and four single fibres were combined on the same graph by plotting the capillary force F_c (mN) against the nominal wetted perimeter (m). Thanks to this graphical representation (Figure 5), it is possible to determine a representative value of contact angle for each test liquid as the slope of the linear fit (resulting from the product of the liquid surface tension and the cosine of contact angle (Eq. **(1)**) [22]. **Figure 5** shows the specific results of carbon and basalt fibres obtained with water. In each case, the linear fit for the advancing, the static and the receding contact angle were plotted taking into account the average capillary force F_c obtained for five tests (section 2.2.2.).

The representation of the slopes of contact angles, for all type of fibres, is quite similar. The advancing and the static contact angles are relatively close, in

comparison to the receding data. Relative difference from the static contact angle in water are of 9% ± 3 and 37% ± 8 for the advancing and the receding angle respectively. The two values of angles, obtained from the best fit possible and the best fit possible including the origin of axes, are used to calculate the dispersion summarized in **Table 2**. As expected from theory of wetting, the relation $\theta_a > \theta_s > \theta_r$ was found to be respected. During the receding phase, a Cos θ > 1 (corresponding to 0-degree contact angle) is often calculated from experimental data, and in every case for fibres in contact with vinylester. The affinity between this resin and the fibres seems to be high because the static and receding contact angles were found to be low or null. The displacement speed is probably in cause, the liquid completely spreads on the fibre surface and a film is formed, which hinders the interpretation of results [6] [21]. This phenomenon, consisting into a transition from partial to total wetting was previously observed in literature and described by the Landau-Levich law [31]. During the fibres receding phase, a dragging of the liquid through the formation of a thin film is observed which have direct consequences on the meniscus mass recorded by the tensiometer and then on the capillary force F_c that will be greater. Qiu *et al.* [29] did not take into account this phenomenon when they suggested to measure contact angles at 20 mm/min.

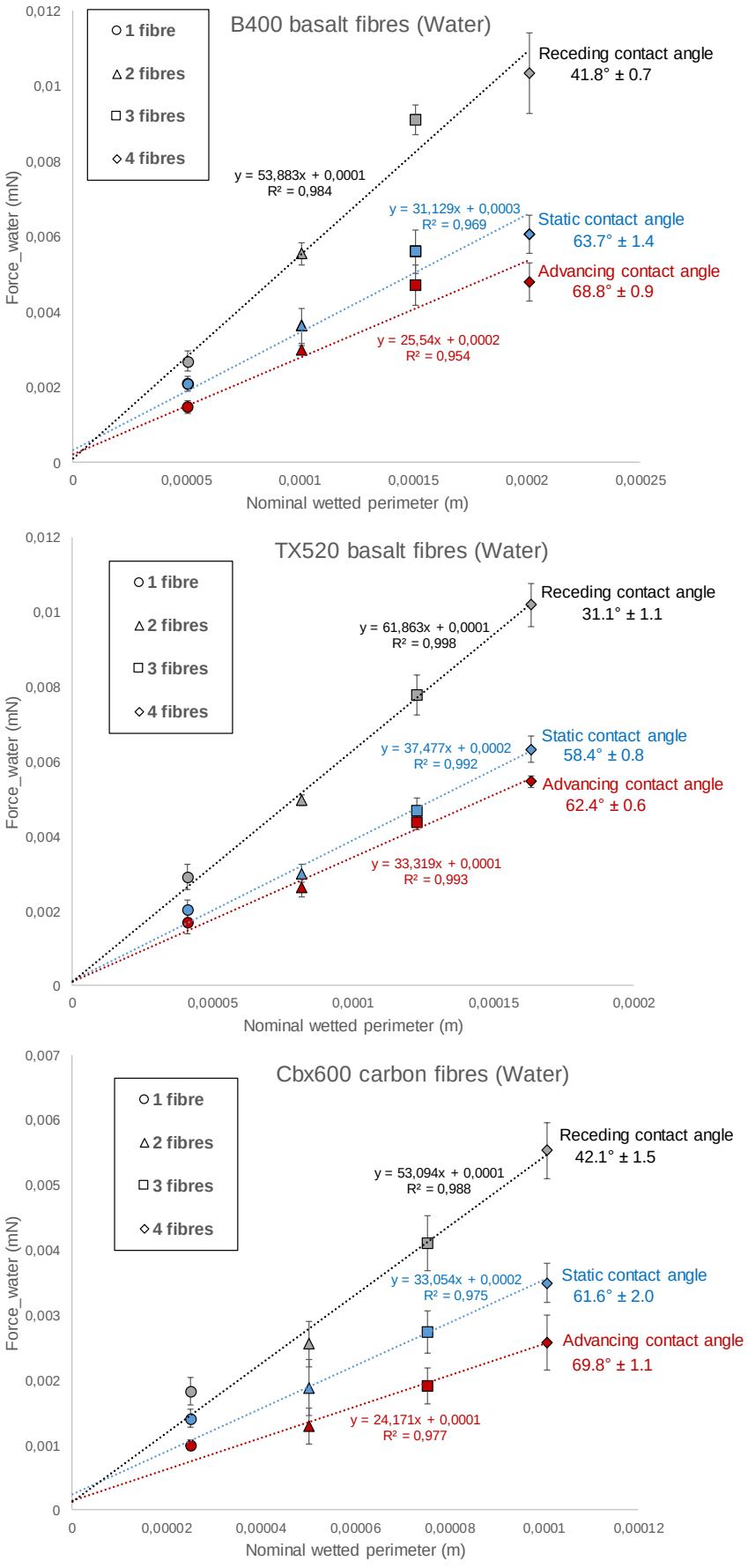

Figure 5. Measurements of contact angles in water for B400 basalt fibres, TX520 basalt fibres and Cbx600 carbon fibres

Table 2. Static, advancing and receding contact angles derived from measurements on basalt and carbon fibres with different liquids and resins.

Fibres	Liquids	$\theta°_s$ / **R²**	$\theta°_a$ / **R²**	$\theta°_r$ / **R²**
Basalt TX520	Water	58.4±0.8 / **0.992**	62.4±0.6 / **0.993**	31.1±1.1 / **0.998**
	SP106	40.9±1.6 / **0.995**	51.0±1.2 / **0.990**	33.9±3.5 / **0.980**
	Vinylester	Cos θ > 1 / **0.992**	23.6±3.1 / **0.964**	Cos θ > 1 / **0.983**
Basalt B400	Water	63.7±1.4 / **0.969**	68.8±0.9 / **0.954**	41.8±0.7 / **0.984**
	SP106	41.9±0.3 / **0.996**	53.0±0.3 / **0.998**	30.9±1.8 / **0.997**
	Vinylester	23.8±4.8 / **0.972**	41.8±3.8 / **0.955**	Cos θ > 1 / **0.954**
Carbon Cbx600	Water	61.6±2.0 / **0.975**	69.8±1.1 / **0.977**	42.1±1.5 / **0.988**
	SP106	28.1±3.1 / **0.984**	42.7±1.7 / **0.990**	Cos θ > 1 / **0.988**
	Vinylester	Cos θ > 1 / **0.983**	Cos θ > 1 / **0.995**	Cos θ > 1 / **0.967**

Moreover, it is important to observe that, whatever the tensiometric method used (DCAT11 or K100SF), the results point in the same direction and can be added or combined to one another. Another important conclusion that can be drawn from Table 2 is that it is possible to achieve a very low dispersion with liquid resin (which is quite an issue with direct optical measurements). It is half the dispersion of what is expected on recent studies on direct measurement [35]. However, results highlight the significant influence of the choice of contact angle calculation (static, advancing and receding). Since the advancing and receding contact angles depend respectively on advancing and receding velocity, only static angles should be considered for surface energy estimation. But, since the aim here is to evaluate the error in surface energies values induced by errors in the contact angle calculation from experimental data, contact angles from dynamic conditions will also be used in an equivalent surface energy calculation.

3.3. Determination of fibre surface energy

Based on the liquid dispersive and polar components (**Table 1**) and knowing contact angles with different liquids and resins, a linear relationship (equation 4) according to the Owens and Wendt method [23] can be established in order to determine the dispersive and polar components of basalt and carbon fibres. **Figure 6** shows plots obtained with values of contact angles following the Owens and Wendt method for three liquids (two resins and water, section 2.1.2.). The theoretical point representing a null angle for n-hexane has also been plotted to take advantage of all the data in the linear regression [22][28]. A good correlation between the experimental results and the Owens and Wendt (OW) relationship was obtained, with correlation coefficients higher than 0.99, independently on the advancing, receding or static contact angles. Surface energies and their components calculated from the OW method are summarized in **Table 3**. Again, as for **Table 2**, calculations on surface energy have been made with OW from angles estimated from the two fits (best fit possible and best fit possible including the origin). Values presented in **Table 3** are then a mean from the two calculated surface energies and components, allowing to also give a dispersion. However, only the static contact angle, being ideally the closest to the equilibrium contact angle, can be considered as valid for the surface energy determination. The Owens and Wendt method (Eq. **(2)**) [23] is derived from the Young-Laplace equation (Eq. **(3)**) [9] which gives only one equilibrium contact angle for a pure liquid. According to some authors [32], the advancing contact angle is associated with an increase in the liquid / solid contact area from a dry state to a wet state, while the receding contact angle is associated to a wet decreasing contact area and to the formation of a thin film in surface. Consequently, considering the dynamic advancing contact angle, as is often the case [8,13,29,33,34], or the receding contact angle is not correct. The lack of data collected, associated with the tensiometric methods usually used, contributes to issues to obtain an equilibrium

contact angle value. An error in the determination of the static contact angle will generate an error in the calculation of the polar and dispersive components and therefore on the total surface energy. Considering the static phase with the DCAT11 tensiometer as well the average of the sum of receding and advancing capillary forces with the K100SF tensiometer, the static contact angle can be determined. This was confirmed through the linear relation of **Figure 6**.

From Table 3 it is relevant to observe that, whatever the fibre considered, the dispersive component is weakly impacted by the choice of the contact angle with an average relative deviation of 7%. On the other hand, the use of a different contact angle (static, advancing or receding) tends to significantly modify the value of surface energy calculated value and more prominently its polar component with an average relative deviation of 51%. There is no modification of the dispersive component of basalt fibres whatever the sizing considered with values of 18.80 ± 0.12 mN/m and 18.89 ± 0.06 mN/m respectively. B400 Basalt fibres compatible with vinylester resins show a weaker polar component. This points out that they will theoretically have better wettability with mainly dispersive resins during LCM process. To further improve the results and decrease dispersion of values determined by OW method, other liquids can be used such as the diiodomethane or the ethylene glycol.

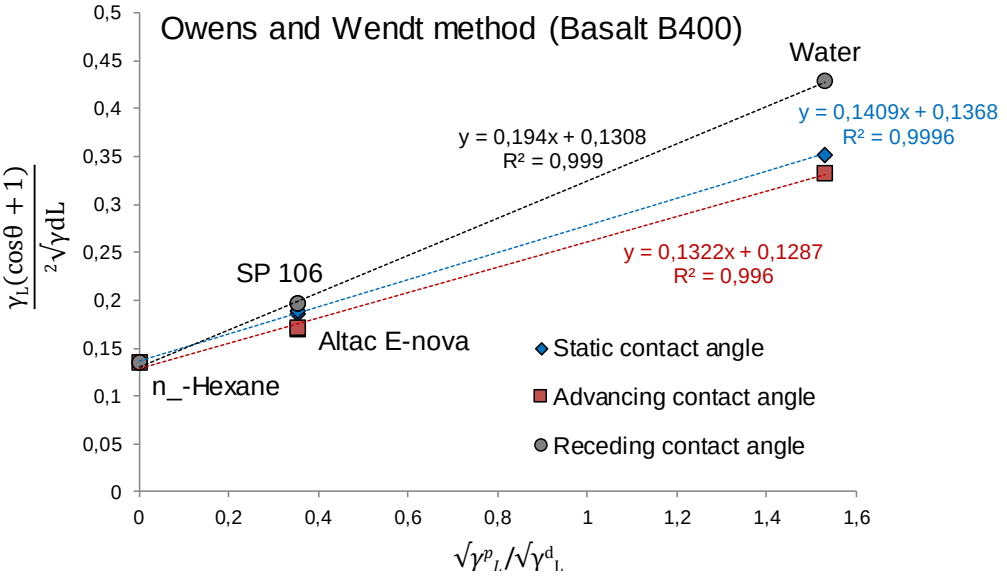

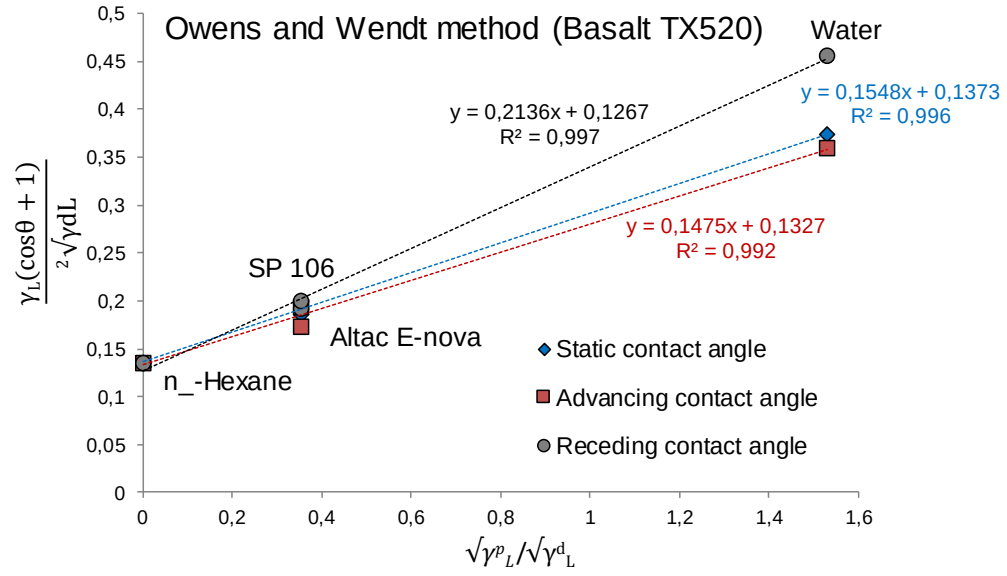

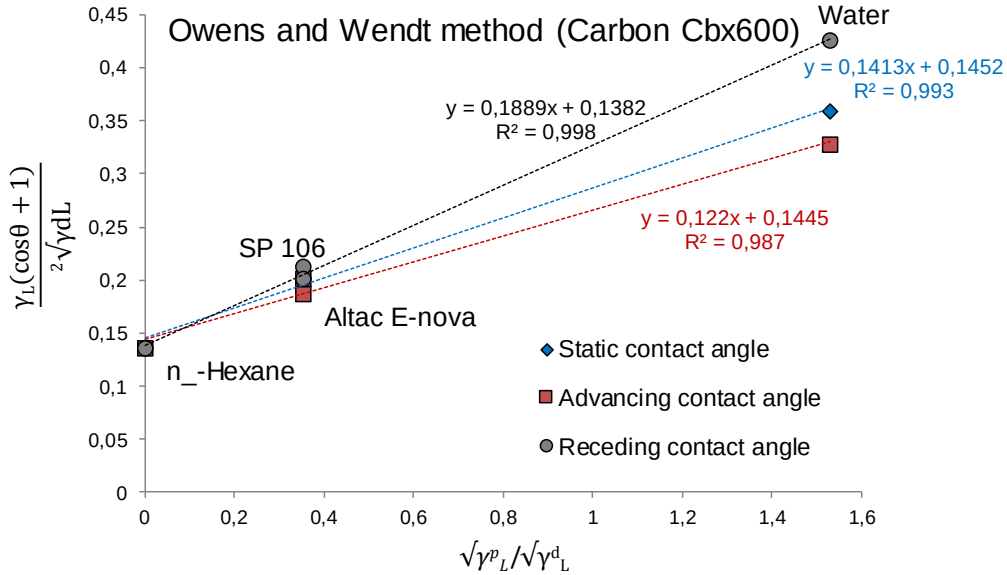

Figure 6. Linear fits for basalt and carbon fibres surface energies as a function of contact angle.

Table 3 Surface energies, of basalt and carbon fibres surface energies as a function of contact angle.

	Contact angle	γ_S^p (mN/m)	γ_S^d (mN/m)	γ_S (mN/m)
Basalt B400	Static	20.54 ± 0.97	18.80 ± 0.12	39.34 ± 1.09
	Advancing	17.84 ± 0.51	16.67 ± 0.27	34.51 ± 0.78
	Receding	37.81 ± 0.25	17.36 ± 0.35	55.17 ± 0.60
Basalt TX520	Static	24.35 ± 0.55	18.89 ± 0.06	43.24 ± 0.61
	Advancing	22.14 ± 0.55	17.50 ± 0.15	39.64 ± 0.70
	Receding	45.97 ± 0.49	16.21 ± 0.22	62.18 ± 0.71
Carbon Cbx600	Static	18.41 ± 1.60	20.65 ± 0.61	39.06 ± 2.21
	Advancing	15.52 ± 0.90	20.59 ± 0.41	36.11 ± 1.31
	Receding	36.52 ± 1.19	18.95 ± 0.21	55.47 ± 1.40

4. Conclusion

The main contribution of this study was to assess the difficulty in determining the equilibrium contact angle by conventional tensiometric method and the repercussions on the calculation of fibres surface energies. To discriminate the device and the measurement methodology, two tensiometric methods from two laboratories were used. The results were combined and the linear regression method, allowing determination of a unique value of contact angle for each couple fibre/liquid, was used. It enhances the reliability of the measurement and minimizes the associated errors. The static, advancing and receding contact angles were determined for each

case and a relative error compared to the theoretical static contact angle was estimated. Issues caused by the need to accurately measure a static contact angle, that will be the closer to the ideal equilibrium conditions, have been highlighted. The associated OW method therefore requires setting a homogeneous methodology for measuring contact angles using tensiometric method. The current method, mainly employed in literature and suggesting that dynamic advancing contact angles measured below 20 mm/min with the K100SF tensiometer can be recognized as static contact angles, is not correct, and causes significant errors, especially for fibres usually submitted to treatments modifying their surface and wettability. A change in the processing of data to consider the angle at equilibrium must be made. Other methods used in literature for the characterization of solid surface energies, such as the sessile drop one, are not suitable for single fibres geometry. Many parameters must be taken into account, as the quality of the photography and the digital processing and a lot of measurement inaccuracies can lead to results being most often far from reality. The rigorous method presented in this study allows drawing the conclusion that B400 and Cbx600 have a very similar surface energy due to their sizing. It proves that despite the differences in term of fibres nature and morphology, the method allows to gather information on the actual behaviour of the sizing. This is of first interest, since estimation of carbon fibres surface energy is rather difficult due to their small size. This method should then be considered at large scale on surface energy characterisation of fibres.

References

[1] Kong X, Hu Y, Wang X, Pan W. Effect of surface morphology on wettability conversion. J Adv Ceram 2016;5:284–90. https://doi.org/10.1007/s40145-016-0201-5.

[2] Lee E, Lee C, Chun Y-S, Han C, Lim D-S. Effect of hydrogen plasma-mediated

surface modification of carbon fibers on the mechanical properties of carbon-fiber-reinforced polyetherimide composites. Compos Part B Eng 2017;116:451–8. https://doi.org/10.1016/J.COMPOSITESB.2016.10.088.

[3] Wu Q, Zhao R, Zhu J, Wang F. Interfacial improvement of carbon fiber reinforced epoxy composites by tuning the content of curing agent in sizing agent. Appl Surf Sci 2020;504:144384. https://doi.org/10.1016/J.APSUSC.2019.144384.

[4] Liu F, Shi Z, Dong Y. Improved wettability and interfacial adhesion in carbon fibre/epoxy composites via an aqueous epoxy sizing agent. Compos Part A Appl Sci Manuf 2018;112:337–45. https://doi.org/10.1016/J.COMPOSITESA.2018.06.026.

[5] Li Y, Wang J, Yang Y, Hamada H, Qiu Y. Surface modifications on basalt fibers. ICCM Int Conf Compos Mater 2013;2013-July:3961–8.

[6] Agrawal G, Negi YS, Pradhan S, Dash M, Samal SK. Wettability and contact angle of polymeric biomaterials. Charact. Polym. Biomater., Woodhead Publishing; 2017, p. 57–81. https://doi.org/10.1016/b978-0-08-100737-2.00003-0.

[7] Chibowski E. On some relations between advancing, receding and Young's contact angles. Adv Colloid Interface Sci 2007;133:51–9. https://doi.org/10.1016/j.cis.2007.03.002.

[8] Park J, Pasaogullari U, Bonville L. Wettability measurements of irregular shapes with Wilhelmy plate method. Appl Surf Sci 2018;427:273–80. https://doi.org/10.1016/j.apsusc.2017.08.186.

[9] Young T. An Essay on the Cohesion of Fluids. Philos Trans R Soc London 1805:65–87. https://doi.org/10.5962/bhl.title.36978.

[10] Van De Velde K Van, Kiekens P. Wettability and surface analysis of glass

fibres. Indian J Fibre Text Res 2000;25:8–13.

[11] Grundke K, Uhlmann P, Gietzelt T, Redlich B, Jacobasch H-J. Studies on the wetting behaviour of polymer melts on solid surfaces using the Wilhelmy balance method. Colloids Surfaces A Physicochem Eng Asp 1996;116:93–104. https://doi.org/10.1016/0927-7757(96)03624-2.

[12] Jafari M, Jung J. The change in contact angle at unsaturated CO2-water conditions: Implication on geological carbon dioxide sequestration. Geochemistry, Geophys Geosystems 2016;17:3969–82. https://doi.org/10.1002/2015GC006171.Received.

[13] Wang J, Fuentes CA, Zhang D, Wang X, Van Vuure AW, Seveno D. Wettability of carbon fiber tows. ICCM Int Conf Compos Mater 2017;2017-Augus:20–5.

[14] Islam MS, Tong L, Falzon PJ. Influence of metal surface preparation on its surface profile, contact angle, surface energy and adhesion with glass fibre prepreg. Int J Adhes Adhes 2014;51:32–41. https://doi.org/10.1016/J.IJADHADH.2014.02.006.

[15] Pucci MF, Liotier PJ, Drapier S. Capillary wicking in a fibrous reinforcement - Orthotropic issues to determine the capillary pressure components. Compos Part A Appl Sci Manuf 2015;77:133–41. https://doi.org/10.1016/j.compositesa.2015.05.031.

[16] PUCCI, M. F., LIOTIER, P.-J., SEVENO, D., *et al.* Wetting and swelling property modifications of elementary flax fibres and their effects on the Liquid Composite Molding process. *Composites Part A: Applied Science and Manufacturing*, 2017, vol. 97, p. 31-40.

[17] Decker EL, Frank B, Suo Y, Garoff S. Physics of contact angle measurement. Colloids Surfaces A Physicochem Eng Asp 1999;156:177–89. https://doi.org/10.1016/S0927-7757(99)00069-2.

[18] Wei J, Zhang Y. Application of Sessile Drop Method to Determine Surface Free Energy of Asphalt and Aggregate. J Test Eval 2012;40:20120060. https://doi.org/10.1520/jte20120060.

[19] Alnoush W, Sayed A, Alyafei N. Optimization of contact angle and interfacial tension measurements for fluid/rock systems at ambient conditions. MethodsX 2019;6:1706–15. https://doi.org/10.1016/J.MEX.2019.07.009.

[20] Pucci MF, Liotier P-J, Drapier S. Capillary effects on flax fibers – Modification and characterization of the wetting dynamics. Compos Part A Appl Sci Manuf 2015;77:257–65. https://doi.org/10.1016/J.COMPOSITESA.2015.03.010.

[21] Pucci, M. F., Duchemin, B., Gomina, M., *et al.* Temperature effect on dynamic wetting of cellulosic substrates by molten polymers for composite processing. *Composites Part A: Applied Science and Manufacturing*, 2018, vol. 114, p. 307-315.

[22] Pucci MF, Liotier PJ, Drapier S. Tensiometric method to reliably assess wetting properties of single fibers with resins: Validation on cellulosic reinforcements for composites. Colloids Surfaces A Physicochem Eng Asp 2017;512:26–33. https://doi.org/10.1016/j.colsurfa.2016.09.047.

[23] Owens DK, Wendt RC. Estimation of the surface free energy of polymers. J Appl Polym Sci 1969;13:1741–7. https://doi.org/10.1002/app.1969.070130815.

[24] Carré A. Polar interactions at liquid/polymer interfaces. J Adhes Sci Technol 2007;21:961–81. https://doi.org/10.1163/156856107781393875.

[25] C. Rulison. Wettability studies for porous solids including powders and fibrous materials. Tech Note, Krus Lab 1999;302:1–14.

[26] Lam CNC, Ko RHY, Yu LMY, Ng A, Li D, Hair ML, et al. Dynamic Cycling Contact Angle Measurements: Study of Advancing and Receding Contact Angles. J Colloid Interface Sci 2001;243:208–18.

https://doi.org/10.1006/JCIS.2001.7840.

[27] Vega MJ, Gouttière C, Seveno D, Blake TD, Voué M, De Coninck J, et al. Experimental investigation of the link between static and dynamic wetting by forced wetting of nylon filament. Langmuir 2007;23:10628–34. https://doi.org/10.1021/la701390m.

[28] Pucci MF, Seghini MC, Liotier P-J, Sarasini F, Tirilló J, Drapier S. Surface characterisation and wetting properties of single basalt fibres. Compos Part B Eng 2017;109:72–81. https://doi.org/10.1016/J.COMPOSITESB.2016.09.065.

[29] Qiu S, Fuentes CA, Zhang D, Van Vuure AW, Seveno D. Wettability of a single carbon fiber. Langmuir 2016;32:9697–705. https://doi.org/10.1021/acs.langmuir.6b02072.

[30] Vander Wielen LC, Östenson M, Gatenholm P, Ragauskas AJ. Surface modification of cellulosic fibers using dielectric-barrier discharge. Carbohydr Polym 2006;65:179–84. https://doi.org/10.1016/J.CARBPOL.2005.12.040.

[31] Landau L, Levich B. Dragging of a Liquid by a Moving Plate. Dyn Curved Front 1988:141–53. https://doi.org/10.1016/B978-0-08-092523-3.50016-2.

[32] Carrier O, Bonn D. Contact Angles and the Surface Free Energy of Solids. Droplet Wetting and Evaporation, Academic Press; 2015, p. 15–23. https://doi.org/10.1016/b978-0-12-800722-8.00002-3.

[33] Wang J, Fuentes CA, Zhang D, Wang X, Van Vuure AW, Seveno D. Wettability of carbon fibres at micro- and mesoscales. Carbon N Y 2017;120:438–46. https://doi.org/10.1016/J.CARBON.2017.05.055.

[34] Lee Y-N, Chiao S-M. Visualization of Dynamic Contact Angles on Cylinder and Fiber. J Colloid Interface Sci 1996;181:378–84. https://doi.org/10.1006/JCIS.1996.0394.

[35] Bénéthuilière, T., Duchet-Rumeau, J., Dubost, E., Peyre, C., & Gérard, J. F. (2020). Vinylester/glass fiber interface: Still a key component for designing new styrene-free SMC composite materials. *Composites Science and Technology*, *190*, 108037.

[36] Pucci, M., Duchemin, B., Gomina, M., & Bréard, J. (2020). Dynamic wetting of molten polymers on cellulosic substrates: model prediction for total and partial wetting. *Frontiers in Materials*, *1*.